Title
Effects of macromolecular configuration of thermally sensitive binder in lithium-ion battery

Journal
Journal of Applied Polymer Science, 134(31)

ISSN
0021-8995

Authors
Le, Anh V
Wang, Meng
Noelle, Daniel J
et al.

Publication Date
2017-08-15

DOI
10.1002/app.45078

Peer reviewed

Journal of Applied Polymer Science

Effects of macromolecular configuration of thermally sensitive binder in lithium-ion battery

Anh V. Le,[1] Meng Wang,[1] Daniel J. Noelle,[2] Yang Shi,[2] Hyojung Yoon,[3] Minghao Zhang,[3] Y. Shirley Meng,[3] Yu Qiao[1,2]

[1]Department of Structural Engineering, University of California—San Diego, La Jolla, California 92093-0085
[2]Program of Materials Science and Engineering, University of California - San Diego, La Jolla, California 92093
[3]Department of Nanoengineering, University of California—San Diego, La Jolla, California 92093
Correspondence to: Y. Qiao (E-mail: yqiao@ucsd.edu)

ABSTRACT: In order to suppress heat generation of nail-penetrated lithium-ion battery (LIB) cell, thermally sensitive binders (TSB) based on poly(vinylidenefluoride) (PVDF) and poly(vinylidenefluoride-*co*-hexafluoropropylene) (PVDF-HFP) were investigated. The testing data showed that with appropriate treatment, TSB could efficiently reduce the peak temperature associated with internal shorting, and did not influence the cycling performance of LIB. The molecular weight of TSB was not a vital factor, while crosslinking was critical. This technology can be used to mitigate thermal runaway of LIB, enabling safe and robust large-scale energy storage. © 2017 Wiley Periodicals, Inc. J. Appl. Polym. Sci. **2017**, *134*, 45078.

KEYWORDS: batteries and fuel cells; composites; thermal properties

Received 11 January 2017; accepted 24 February 2017
DOI: 10.1002/app.45078

INTRODUCTION

To power long-range electric vehicles (EV), lithium-ion batteries (LIB) are currently being extensively investigated.[1] The studies are often focused on novel architectures and nanostructures of high-energy electrodes.[2] A number of active materials as well as electrolytes have been developed to improve the specific energy and the cycle life.[3] Another major concern of EV batteries is their robustness and safety. Today's LIB cells contain highly flammable electrolytes, and in case of vehicle collision, LIB may undergo thermal runaway.[4] Associated with internal shorting, local temperature in LIB can rapidly increase and the structure may catch fire in less than a few minutes.[5] A number of system-level approaches are under investigation to protect the driver and the LIB packs. In these designs, heavy auto frame components are often utilized for impact energy absorption. Such a system imposes tight constraints on the rigidity, placement, cell spacers, and vertical and lateral supports of LIB packs, and is heavy and large, significantly reducing the overall specific energy.[6] Moreover, the protection system is capable of protecting the batteries only at the pack level. In an intense vehicle collision, as LIB cells are mechanically abused,[7] positive and negative electrodes may come into contact with each other, creating an internal path of direct flow of charges and triggering a series of rapid exothermic reactions.[8] The local temperature can reach ~300 °C within 1 min, sufficient to damage the separators in neighboring cells.[9] It is highly desirable that thermal-runaway mitigation (TRM) mechanisms can be inherently built into the LIB cells.

Traditional cell-level TRM approaches include safety vents, shutdown separators, non-flammable electrolytes, etc.[10] While these methods can reduce fire hazard under certain conditions, they also have considerable limitations. The pore-closing mechanism of shutdown separators would become less effective once the separators are broken apart. For the past couple of decades, a group of additives classified as positive temperature coefficient (PTC) materials have gathered great attention.[5,10] A PTC material is designed such that phase transition takes place as the temperature reaches 125–150 °C at the local shorting site, which allows a significant volume expansion to cut off the ion/electron transportation; thus, heat generation is reduced. A somewhat similar method is to add damage homogenization (DH) additives in electrodes.[11–13] When the electrode is damaged, the DH additives promote widespread cracking and debonding, which separates the internal short site from the surrounding active materials. One issue of the PTC and DH additives is that the manufacturing procedure of LIB may be adjusted, which affects industrial engineering, quality control, and cost.

Usually, a LIB electrode is formed by binding active material particles with a polymer binder. The active material particle size is typically 5–20 μm, and the binder content is 3–5 wt %. The

binder must be relatively strong, wetting well to the active materials, highly processable, and highly durable in the harsh LIB environment. Commonly employed binders include poly(vinylidene fluoride) (PVDF) for cathode and carboxymethyl cellulose (CMC) and styrene butadiene rubber (SBR) mixture for anode.[14] It is envisioned that if the polymer binder of LIB electrode is thermally sensitive, the internal impedance of LIB cell could be largely increased after internal short circuits are formed, which suppresses thermal runaway. The slurry processing could be similar to the conventional procedure, and the cell mass does not vary, i.e., the specific energy remains the same. The thermally sensitive binder (TSB) is designed to fail at elevated temperature (~110 °C) and to disintegrate the electrode components. Our previous testing results showed a 40% reduction in peak temperature increase in nail penetration test on coin cells[15]; however, the cycle life of these TSB-based LIB was poor, which was attributed to the premature swelling of the investigated TSB, poly(vinylidenefluoride-*co*-hexafluoropropylene) (PVDF-HFP). The HFP component renders the binder phase thermally sensitive yet also more amorphous and more susceptive to electrolyte attack. Even though the ability to absorb electrolyte enhances the ionic conductivity, it is only favorable when the material is used as the membrane separator, and only with a low HFP content less than 24 wt %.[16,17] When the HFP content is above 30 wt %, PVDF-HFP absorbs much electrolyte, swells, and loosens the contact among the particles of active materials and current collector. In addition, the more access the electrolyte has to the active materials, the more side reactions would occur, forming thicker solid-electrolyte-interphase (SEI) layers. Because SEI does not conduct electrons and is nearly impenetrable to electrolyte, the electrode becomes less conductive both ionically and electronically.

In order to enhance the cycle life of TSB-based LIB, in the current study we investigated the effects of molecular weight (M_W) and crosslinking of the polymer binder. The TSB must maintain its high processability and have little detrimental effects to the performance of other LIB components, i.e., active materials, carbon black (CB), and electrolyte. The TSB should be strong at room temperature and disintegrate the electrode at 100–130 °C, since the onset temperature of thermal runaway of LIB is ~150 °C.[4,5]

EXPERIMENTAL

Battery Cell Processing and Testing

For cathode, the active material (AM) was a high-energy lithium nickel manganese oxide, NMC532 (NCM-04ST from TODA America, Battle Creek, MI). The average particle size of NMC532 was about 10 μm. The reference binder (B) was PVDF, with the molecular weight, M_W, of either 534,000 g/mol (Sigma-Aldrich, Product No. 182702) or 180,000 g/mol (Kynar PVDF Grade 711); they will be respectively referred to as B01 and B02 in the following discussion. The TSB was a PVDF-HFP with the HFP content of 32 wt % (Kynar Flex 2500-20), which will be referred to as B03. The carbon black (CB) nanoparticles were TIMCAL CNERGY-C65. The mass ratio among the components was AM:B:CB = 93:4:3, typical for LIB coin cells. 1-Methyl-2-pyrrolidone (NMP) (product no. 328634 from Sigma-Aldrich) was used as solvent for the slurry processing. The AM, CB, and binder powders were thoroughly dissolved or suspended in NMP to obtain a viscous slurry. The slurry was cast on a 17-μm-thick aluminum foil, dried in a vacuum oven for 24 h, and compacted to the final thickness. The dried electrode film was cut into small discs of 1.43 cm diameter. The mass of AM was approximately 7–8 mg/cell for cycle life testing, and 35–40 mg/cell for nail penetration testing. In each coin cell, a lithium metal disc of 1.43 cm diameter and 1.1 mm thickness was used as the anode; a 25-μm-thick highly porous trilayer membrane (Celgard, Charlotte, NC, Product No. 2325) was used as the separator; and the electrode stack was enclosed in a CR2016 stainless steel cell case.

To test the cycling performance, the cell was charged and discharged between 4.3 and 3.0 V at 60 °C, by using an 8-channel battery analyzer (MTI BST8-3). The cell was placed in an oven chamber, connected to a DigiTrol II temperature controller (Sigma-Aldrich, product no. Z285498). The elevated temperature accelerated aging of the electrode, while was still within the safe range.[18] The first cycle was performed at a low current rate, 0.1 C, to establish stable SEI. The following cycles were performed at 1 C rate.

For nail penetration testing, the LIB cell was first charged–discharged between 3.0 and 4.2 V for five cycles at 1 C, and then fully charged to 4.6 V, by using the same Battery Analyzer. The charged coin cell was pre-heated at 110 °C for 1 min on a hot plate (Corning PC 4000), and air-cooled to ambient temperature. The pre-heated coin cell was rested for ~10 min, and its voltage was typically in the range from 4.44 to 4.46 V; the final capacity was approximately 5 mAh. Figure 1 depicts the nail penetration experimental setup. A coin cell was insulated by a polyurethane (PU) foam and penetrated by a steel nail at the center. The temperature was measured by an Omega TT-K-40-25 (type-K gage 40) thermocouple, equipped with an Omega OM-EL-USB-TC temperature logger. The thermocouple was ~2.5 mm away from the nail. The nail was made of type 316 stainless steel. The length and diameter of the nail were 12.7 mm and 1.59 mm, respectively. The thermal conductivity was approximately 17 W/(m K). The speed of nail penetration was ~1.6 mm/s.

Treatment of Thermally Sensitive Polymer Binders

Binders with Controlled Molecular Weight. Table I lists the cathode binders under investigation. The reference binders were B01, B02, and B03; the rest were treated polymer binders.

Molecular weight, M_W, is a vital factor that dominates thermal, mechanical, and swelling properties of polymers.[19] Previous testing data indicated that the solvent resistance of B03 was too low while the softening temperatures of B01 and B02 were too high.[15] Therefore, if M_W of B03 can be increased or M_W of B01 or B02 can be reduced, the balance between thermal sensitivity and swelling might be enhanced.

To vary M_W of polymer binder while keeping everything else as constant as possible, we harvested binder samples from the reference polymers through controlled precipitation. About 10 g of B01, B02, or B03 was first dissolved in 100 mL of acetone. In a

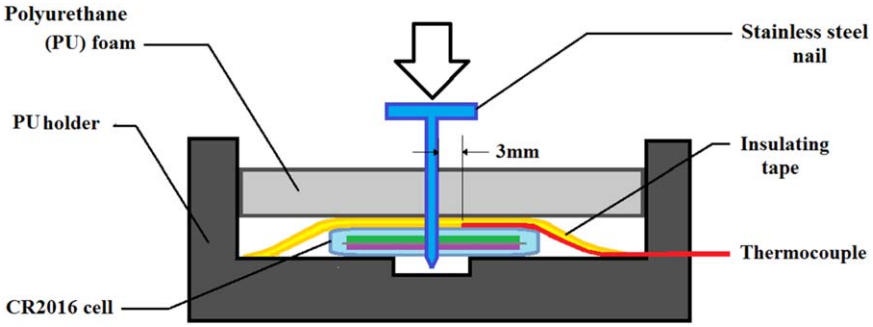

Figure 1. Schematic of the nail penetration testing setup. [Color figure can be viewed at wileyonlinelibrary.com]

capped beaker, the solution was stirred continuously at 1000 rpm with a mechanical stirrer (IKA EUROSTAR 20) for 1 h; the beaker was placed on a hot plate (Corning PC 4000), with the temperature set to 100 °C. The solution was then transferred to an open container and placed back onto the heater, so that acetone evaporated. Polymer precipitate was visible after about 5 min, and was collected every 5 min by using a stainless-steel tweezer, until the remnant material became gel-like. The harvested precipitate tended to have a higher M_W than the remnant material.[20] As similar controlled-precipitation processes were repeated for harvested or remnant materials, the highest-M_W and the lowest-M_W portions of polymer were separated. The final harvested material was 6 wt % (B01), 2 wt % (B02), or 0.5 wt % (B03) of the initial polymer. The harvested binders were used for the slurry processing of electrodes.

Crosslinked Binders. When properly formed, crosslinks could strengthen polymer and improve the resistance to swelling.[21] PVDF-HFP can be crosslinked by bisnucleophiles, such as diamines or bisphenols, peroxides, or by irradiation.[22] Common crosslinking agents include hexamethylene diamine (HMDA) and their carbamates (HMDA-C) or derivatives, benzoyl peroxide (BPO), etc.[22] Bisphenols and diamines would produce hydrofluoric acid (HF) or require co-agents that have detrimental effects on active materials.[23] In the current study, BPO (Luperox A75, obtained from Sigma-Aldrich, product code 1001522084) was employed, following an established procedure[24]: BPO was dissolved in NMP and mixed with other components of electrode; the amount of BPO is shown in Table I. After drying, the electrode film was compressed at 5 MPa using a type-5582 Instron machine for 5 min, to stabilize the microstructure; and then sandwiched in between two stainless steel pistons, secured by a C-clamp. The polymer was cured in a Carbolite CFT 12 tube furnace at 200 °C for 2 h. Finally, the electrode film was cut into discs, and used to assemble LIB half-cells.

Differential Scanning Calorimetry

Differential scanning calorimetry (DSC) analysis was conducted to characterize the polymer binders. Polymer films were prepared through solvent casting in NMP. About 2 g of polymer was mixed with 15 mL NMP, forming a gel. The polymer gel was flattened to about 2 mm thick, dried in a VWR 1410 vacuum oven at 80 °C for 24 h, and formed a flexible film ~1 mm thick. The film was cut into 6.35-mm-diameter discs. Each disc weighed ~10 mg, with the final thickness of about 200 μm. DSC scan was performed in the temperature range from 40 to 200 °C, at the scanning rate of 10 °C/min, by using a DSC 8000 machine (Perkin Elmer).

Table I. List of the Cathode Binders under Investigation

Modification method	Binder code	Binder component	
		Component 1	Component 2
	B01	PVDF ($M_W \approx$ 534,000 g/mol)	
	B02	PVDF ($M_W \approx$ 180,000 g/mol)	
	B03	PVDF-HFP with 32 wt % HFP ($M_W \approx$ 500,000 g/mol)	
Controlled molecular weight (M_W)	R1	Low-M_W portion harvested from B01 (6 wt % of B01)	
	R2	Low-M_W portion harvested from B02 (2 wt % of B02)	
	R3	High-M_W portion harvested from B03 (0.5 wt % of B03)	
Crosslinking	X-2	B03	BPO (2 wt % of Component 1)
	X-10		BPO (10 wt % of Component 1)
	X-20		BPO (20 wt % of Component 1)

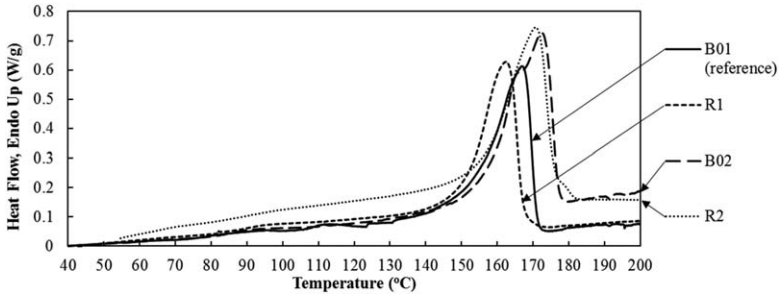

Figure 2. Typical DSC curves of PVDF binders.

RESULTS AND DISCUSSION

In an electric vehicle, a LIB cell stores ~3–40 Ah energy.[24] With such a high capacity, a large amount of heat can be generated when internal shorting takes place, and raise the temperature to ~150 °C rapidly, after which thermal runaway may become uncontrollable.[4,5,25] For the coin cells investigated in the current study, the cell capacity is only ~5 mAh and the surface-to-volume ratio is large; thus, even if all the stored energy is released, the temperature increase is only a few degree centigrade. To simulate the high-temperature environment of a damaged large LIB cell, pre-heating is conducted on the coin cells at 110 °C, the desired temperature at which the binder begins to take effect to mitigate thermal runaway. After preheating, the cell is cooled down for 10 min before proceeding with nail penetration, so that the cell reaches stable temperature and voltage.

Figure 2 shows the DSC measurement results. On the *y*-axis, the upward direction indicates endothermic reaction. The DSC curve of B03 contains broad shoulders for both dry and electrolyte-soaked samples. This thermal response is usually attributed to the wide range of molecular weight. The shorter polymer chains form smaller semi-crystalline areas that melt at lower temperatures; longer chains form larger semi-crystalline areas that melt at higher temperatures.[26,27] Heat of fusion, ΔH_f, is computed for the semi-crystalline PVDF samples (Table 2). A higher value of ΔH_f indicates a higher crystallinity.[26,27]

As shown in Figure 2, melting of dry B03 begins at about 80 °C. When soaked in electrolyte, the polymer becomes less stiff; the melting temperature range is 15–20 °C lower, and the heat absorption is much reduced. More importantly, the electrolyte-soaked B03 is softened at ~50 °C, which explains the poor cycle lives of LIB cells based on pristine B03.[15] Clearly, the as-received B03 offers relatively low strength, low solvent resistance, and low thermal stability. The as-received B03 has a relatively broad M_W distribution, which is likely one of the reasons of the fast degradation rate of LIB coin cells.[15] As the charge–discharge cycles continue, the macromolecules of the lowest M_W lead to aggressive local swelling, so that the overall LIB cell capacity decreases. Through the controlled-precipitation process, we harvest the top 0.5 wt % B03 of high M_W. From Figure 3, it can be seen that even though the high-M_W B03 (R3) leads to a much better cycling performance than B03-based cells, the degradation rate is still must faster than that of B01-based cells, suggesting that while the high M_W improves the strength and the swelling resistance of B03, the binder phase still cannot survive the harsh charge–discharge process. One of the possible reasons of the poor performance of R3 is that PVDF-HFP tends to be highly amorphous.[28]

Table 2. Average Heat of Fusion of PVDF Binders, ΔH_f (J/g)

Binder code	Heat of fusion, ΔH_f (J/g)
B01	44.1
B02	40.3
R1	44.0
R2	38.6

The controlled precipitation operations are also conducted on B01 and B02, to harvest low-M_W portions of them, R1 and R2, that account for 2 wt % and 6 wt % of B01 and B02, respectively. Figure 2 indicates that the peak melting temperatures of R1 and R2 are shifted to the lower end, as they should be. However, the shifts are only a few degree centigrade, quite small compared with the difference between the original peak melting temperatures and the critical point of LIB thermal runaway (~150 °C). The values of heat of fusion also show a minimal difference between the as-received polymers, i.e., B01, B02, and their respective refined material, i.e., R1 and R2. The molecular weight control method is somewhat more effective on B02, as the shift of melting peak and reduction in heat of fusion are more prominent compared to R1 and B01. This is attributed to the relatively low initial molecular weight and low degree of branching of B02, which allows the polymer chains to be better detangled in acetone solvent. Regardless, when the LIB cell is abused, the change in thermal properties of R1 and R2 may not be sufficient to trigger widespread defunctionalization of electrodes before heat generation accelerates, as shown in Figure 4: Upon nail penetration, the peak temperatures of R1 and R2 based LIB cells are quite similar with that of B01-based reference cells, suggesting that the heat generate rate do not vary much.

Crosslinked PVDF-HFP has been used to produce membranes in LIB to host electrolyte.[16,29] Crosslinking PVDF-HFP is relatively difficult under mild conditions.[22] With the presence of lithium metal oxides, carbon black nanoparticles, and electrolyte in the electrode layer, the control on porosity, swelling resistance, and SEI of electrode becomes challenging. In the current study, we use BPO as the crosslinking agent. According to Figure 3, it is clear that compared with un-modified B03,

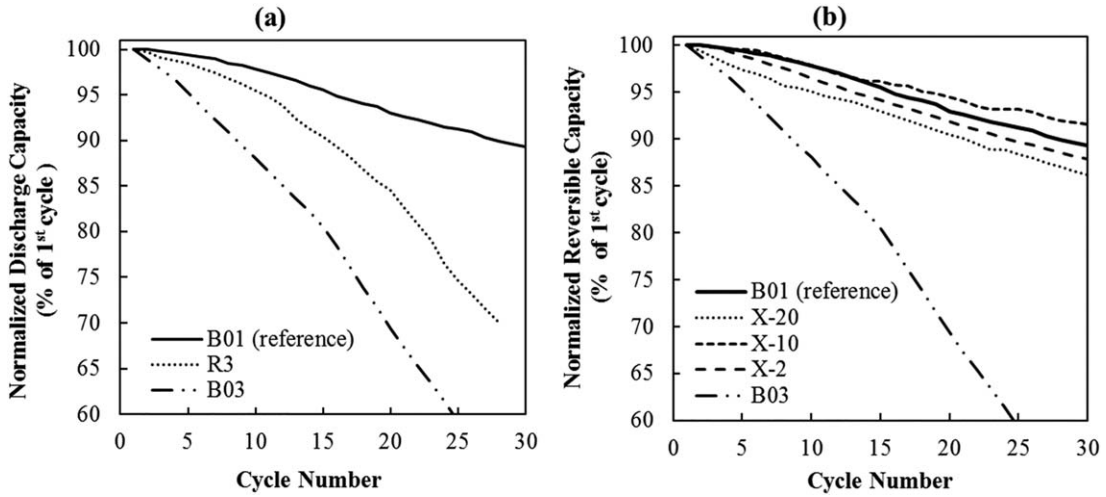

Figure 3. Typical cycling performance of cathode half-cells based on various binders.

crosslinked binders lead to much better cycle lives of LIB cells. The crosslinking process is adjusted by the amount of BPO, typically in the range of a few percent to 15 wt %.[24] In binders X-2, X-10, and X-20, the BPO contents are 2 wt %, 10 wt %, and 20 wt % of B03, respectively. The cycling performance of X-2 based LIB cells is lower, but comparable with that of B01-based reference cells. When the BPO content increases to 10 wt %, X-10 based LIB cells exhibit a better cycle life than reference cells. As the BPO content further rises to 20 wt %, however, the degradation rate of X-20 based cell is increased to higher than that of X-2 based cell, but still much lower than that of the cells based on pristine B03.[15] It is clear that crosslinking helps stabilize the binder phase and reduce swelling, so that the LIB cells are much more stable than B03-based ones. When the BPO content is too high, the crosslinking agent may attack the polymer chains and result in chain scission.[22] Figure 4 shows that in nail penetration test, the temperature increase, ΔT, of X-10 based cell is considerably lower than that of B01-based reference cell by nearly 37%; that is, X-10 is a functional binder that not only may slightly enhances the electrochemical performance of LIB cell during normal operation, but also suppresses heat generation when the cell is mechanically abused. Note that the temperature increase of X-10 based cell is higher than that of B03-based cell, since the stronger X-10 binder renders the electrode layer more structurally integral and the widespread damaging is less extensive at elevated temperature.

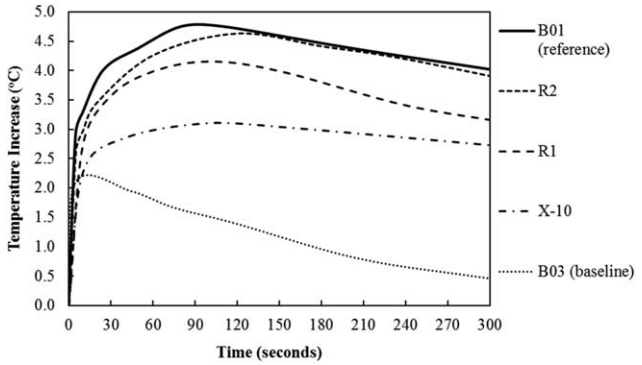

Figure 4. Typical temperature profiles of nail penetration tests on coin cells based on various binders.

Note that in the current study, we focus on LIB half-cells with lithium film anodes. It represents a more severe situation than LIB full cells, as lithium metal tends to be more aggressive than lithiated graphite. For each binder listed in Table I, we tested more than five half-cells and the results were consistent. Testing full cells and large-sized pouch cells will be important tasks of our future work.

CONCLUSIONS

Thermally sensitive binders (TSBs) of lithium-ion battery (LIB) were investigated. The TSBs were based on PVDF-HFP, with controlled molecular weight or crosslinking. Charge–discharge cycling tests and nail penetration tests suggested that controlling molecular weight was relatively inefficient; crosslinking could help enhance the cycling performance under normal working condition and considerably reduce heat generation upon mechanical abuse. These phenomena can be attributed to the effects of macromolecular configuration on the temperature sensitivity and swelling resistance of the polymer binder. The finding may shed light on developing abuse-tolerant high-energy LIB cells.

ACKNOWLEDGMENTS

This research is supported by the Advanced Research Projects Agency—Energy (ARPA-E) under Grant No. DE-AR0000396, for which authors are grateful to Dr. Ping Liu, Dr. John Lemmon, Dr. Grigorii Soloveichik, Dr. Chris Atkinson, and Dr. Dawson Cagle. Special thanks are also due to Dr. Jiang Fan and Dr. Dengguo Wu for the help with lithium-ion battery design and processing

REFERENCES

1. Lu, L.; Han, X.; Li, J.; Hua, J.; Ouyang, M. *J. Power Sources* **2013**, *226*, 272.

2. Sun, Y. K.; Chen, Z.; Noh, H. J.; Lee, D. J.; Jung, H. G.; Ren, Y.; Wang, S.; Yoon, C. S.; Myung, S. T.; Amine, K. *Nat. Mater.* **2012**, *11*, 942.
3. Hasanbeigi, A.; Sathaye, J. Public Interest Energy Research (PIER) Program. Final Project Report. California Energy Balance Update and Decomposition Analysis for the Industry and Building Sectors (No. LBNL–5918E); Lawrence Berkeley National Laboratory (LBNL): Berkeley, CA (United States), **2010**.
4. Roth, E. P.; Orendorff, C. J. *Electrochem. Soc. Interface* **2012**, *21*, 45.
5. Doughty, D.; Roth, E. P. *Electrochem. Soc. Interface* **2012**, *21*, 37.
6. Arora, S.; Shen, W.; Kapoor, A. *Renew. Sustain. Energ. Rev.* **2016**, *60*, 1319.
7. Xia, Y.; Wierzbicki, T.; Sahraei, E.; Zhang, X. *J. Power Sources* **2014**, *267*, 78.
8. Finegan, D. P.; Scheel, M.; Robinson, J. B.; Tjaden, B.; Hunt, I.; Mason, T. J.; Millichamp, J.; Di Michiel, M.; Offer, G. J.; Hinds, G.; Brett, D. J. *Nat. Commun.* **2015**, *6*, 6924.
9. Feng, X.; Sun, J.; Ouyang, M.; Wang, F.; He, X.; Lu, L.; Peng, H. *J. Power Sources* **2015**, *275*, 261.
10. Balakrishnan, P. G.; Ramesh, R.; Kumar, T. P. *J. Power Sources* **2006**, *155*, 401.
11. Williams, J. G. *Compos. Sci. Technol.* **2010**, *70*, 885.
12. Le, A. V.; Wang, M.; Shi, Y.; Noelle, D.; Qiao, Y.; Lu, W. *J. Appl. Phys.* **2015**, *118*, 085312.
13. Le, A. V.; Wang, M.; Shi, Y.; Noelle, D. J.; Qiao, Y. *J. Phys. D: Appl. Phys.* **2015**, *48*, 385501.
14. Chou, S. L.; Pan, Y.; Wang, J. Z.; Liu, H. K.; Dou, S. X. *Phys. Chem. Chem. Phys.* **2014**, *16*, 20347.
15. Le, A. V.; Wang, M.; Noelle, D. J.; Shi, Y.; Yoon, H.; Meng, Y. S.; Wu, D.; Fan, J.; Qiao, Y. Effects of thermal sensitivity of cathode binder on the heat generation of nail-penetrated lithium-ion battery cell. To be published.
16. Song, M. K.; Kim, Y. T.; Kim, Y. T.; Cho, B. W.; Popov, B. N.; Rhee, H. W. *J. Electrochem. Soc.* **2003**, *150*, A439.
17. Raghavan, P.; Zhao, X.; Choi, H.; Lim, D. H.; Kim, J. K.; Matic, A.; Jacobsson, P.; Nah, C.; Ahn, J. H. *Solid State Ionics* **2014**, *262*, 77.
18. Waldmann, T.; Wilka, M.; Kasper, M.; Fleischhammer, M.; Wohlfahrt-Mehrens, M. *J. Power Sources* **2014**, *262*, 129.
19. Nunes, R. W.; Martin, J. R.; Johnson, J. F. *Polym. Eng. Sci.* **1982**, *22*, 205.
20. Ueberreiter, K. The Solution Process. In: Crank, J.; Park, G. S. (Eds.). *Diffusion Polym.* Academic Press: New York, NY, USA; **1968**. pp. 219–257
21. Nielsen, L. E. *J. Macromolecular Sci. Pt C*; **1969**, *3*, 69.
22. Taguet, A.; Ameduri, B.; Boutevin, B. In Abe, A.; Dusek, K.; Kobayashi, S. Crosslinking in Materials Science; Springer: Berlin, Heidelberg, **2005**; p 127.
23. Aurbach, D.; Markovsky, B.; Salitra, G.; Markevich, E.; Talyossef, Y.; Koltypin, M.; Nazar, L.; Ellis, B.; Kovacheva, D. *J. Power Sources* **2007**, *165*, 491.
24. Shen, Q.; Chen, Y.; Cheng, Z.; Liu, L.; Chen, X. Patent CN 102924732 B, Nanjing University, (**2013**).
25. Orendorff, C.; Lamb, J.; Steele, L. A. M.; Spangler, S. W.; Langendorf, J. Quantification of Lithium-ion Cell Thermal Runaway Energetics (No. SAND2016-0486); Sandia National Laboratories (SNL-NM): Albuquerque, NM (United States), **2016**.
26. TA Instruments. Determination of Polymer Crystal Molecular Weight Distribution by DSC [Online]. Available at: http://www.tainstruments.com/pdf/literature/TA276.pdf. [Accessed December 24, 2016].
27. TA Instruments. Thermal Analysis Application Brief - Determination of Polymer Crystallinity by DSC [Online]. Available at: http://www.tainstruments.com/pdf/literature/TA123.pdf. [Accessed December 24, 2016]
28. Ahmed, T. S.; DeSimone, J. M.; Roberts, G. W. *Macromolecules* **2006**, *39*, 15.
29. Katsurao, T.; Horie, K.; Nagai, A.; Ichikawa, Y. Kureha Kaguka Kogyo Kabushiki Kaisha. U.S. Pat. 6,372,388 (**2002**).